DOI: https://doi.org/10.54966/jreen.v26i2.1150 - *Journal of Renewable Energies 26 (2023) 141 – 160*

Journal of Renewable Energies

Revue des Energies Renouvelables

journal home page : https://revue.cder.dz/index.php/rer

Research paper

The thermal and stored heat energy driving a Stirling engine for power generation

Elardus Erasmus Duvenage[a], **Dr Trudy Sutherland** [a*]

[a] *Vaal University of Technology, Andries Potgieter Blvd, Vanderbijlpark, South Africa*

ARTICLE INFO

Article history:
Received June 2, 2023
Accepted October 15, 2023

Keywords:
Photovoltaic,
Solar,
Stored heat energy,
Stirling engine,
MATLAB,
Battery backup

ABSTRACT

South Africa's national power grid is currently in dire straits. The lack of a dependable power supplier and rising electricity costs force the public and businesses to look for alternatives to meet their energy needs. These alternatives are costly to implement and beyond the financial reach of most South Africans. The most common alternative energy source is solar photovoltaic systems with large battery banks to survive Eskom's long, regular load-shedding schedules. This research aims to design and simulate a combined solar-thermal and stored heat energy-powered Stirling engine for power generation. The output of the research simulation was compared to a standard photovoltaic installation of similar power output. The results for this paper were generated from the simulation software package MATLAB. Such a system must have a lower capital cost to compete with solar photovoltaic systems with battery backup. The Stirling system was found to be cheaper than the deep-cycle gel system and about 11% cheaper than the PV system using lithium iron phosphate.

1. INTRODUCTION

"Electricity is essential to innovation, progress and life" (Hughes, 2018). South Africa's national electricity supplier – Eskom – is under severe pressure to supply the country with the electricity it needs to be productive and have a sustainable economy (Mannak, 2015). According to a survey done by independent energy experts, Eskom's Energy Availability Factor (EAF) dropped from 64,79% to

[*] *Corresponding author, trudys@vut.ac.za*
Tel : + 2716 950 9724

ISSN: 1112-2242 / EISSN: 2716-8247

61,75% from 2020 to 2021. EAF is the average amount of Eskom's power generation available compared to its installed capacity (Mileham, 2022). According to the Council for Scientific and Industrial Research (CSIR), 2021 was the worst year on record regarding load-shedding, with 1 136 hours of outages compared to 859 hours recorded in 2020. This is an increase of 37% (Mileham, 2022). To make matters worse, electricity tariffs increased by 753% between 2007 to 2021, whilst inflation was only 134% over the same period. This means that the increase in electricity tariffs is five times higher than inflation (Moolman, 2021). Due to rising electricity prices, load-shedding threats, global warming awareness and decreasing technology costs, small-scale embedded generation investment has become more attractive to residential, commercial and industrial end-user consumers (Pandarum et al., 2019). South Africa is a perfect location for harvesting solar energy, with an average of 2 500 hours of sunshine per year and average solar radiation levels between 4.5 and 6.5kWh/m2 per day (DOE South Africa, 2022). While the statistics on solar photovoltaic (PV) installations in South Africa are based on industry estimates and cannot be regarded as comprehensive or official, it shows that rooftop PV systems are a reality in South Africa (Pandarum et al. 2019). The price of solar PV has dropped by almost 90% between 2010 and 2020 yet installing a grid-tied solar home system for a 3- to 4-bedroom standalone home will still cost between R150 000 and R200 000 (Toussaint, 2020; Chivandire, 2020). Off-grid systems can cost as much as three times more than a grid-tied system (Chivandire, 2020). This means that the initial capital cost of a solar PV system will be too expensive for most South Africans, especially low-income households. This research explores using a Stirling engine driven by concentrated solar thermal energy (CST) and heat energy stored in water for power generation.

2. LITERATURE STUDY

2.1 The Stirling Engine

The Stirling engine (see Fig1) was patented in 1816 by Robert Stirling and is a type of heat engine that is operated by the cyclic compression and expansion of air or other gas (the working fluid) between different temperatures, resulting in a net conversion of heat energy to mechanical work (Walker, 1980; Pendrid, 1917). "Like any heat engine, the Stirling engine goes through the four basic processes of compression, heating, expansion, and cooling" (Martini, 1983). When heat is added to the hot cylinder, the gas inside expands and pushes the piston down; as the gas cools down, the piston returns and pushes the working fluid through the channel towards the cold cylinder. Here the gas is cooled down and compressed by the cold piston and pushed back to the hot cylinder for the process to be repeated (Martini, 1983). The regenerator is between the hot and cold cylinders and acts as an internal heat exchanger. It temporarily stores heat energy from the working fluid as the gas flows from the hot to cold cylinders. When the cycle is reversed, i.e., the gas flows from the cold to hot cylinders, the heat is "released" back into the working fluid (Rinker, 2018).

2.2 Concentrated Solar Power

Concentrated solar power generates electricity by concentrating the sun's heat energy onto a collector, which transfers that energy into a medium (water, air or other working fluid) that drives a conventional power cycle (Hagumimana et al. al. 2021). Concentrated solar power systems comprise concentrators, collectors, thermal energy storage systems and the power block. Concentrators (also called reflectors) are usually made up of mirrors and used to concentrate the sun's heat onto a specific point where a collector is located. Collectors (receivers/absorbers) collect and transfer solar heat energy to a heat transfer fluid or working fluid. The thermal energy storage system stores the thermal energy in a thermal energy storage medium like liquid molten salt, silica sand or other material to use when the sun is not shining. The power block uses the heat transfer fluid to boil water to generate steam which drives steam

turbines to generate electricity (Alalewi, 2014). Concentrated solar power can be divided into 4 types based on structure and how the solar radiation is concentrated: parabolic trough, linear Fresnel reflector, solar tower and parabolic dish (Răboacă et al. 2019).

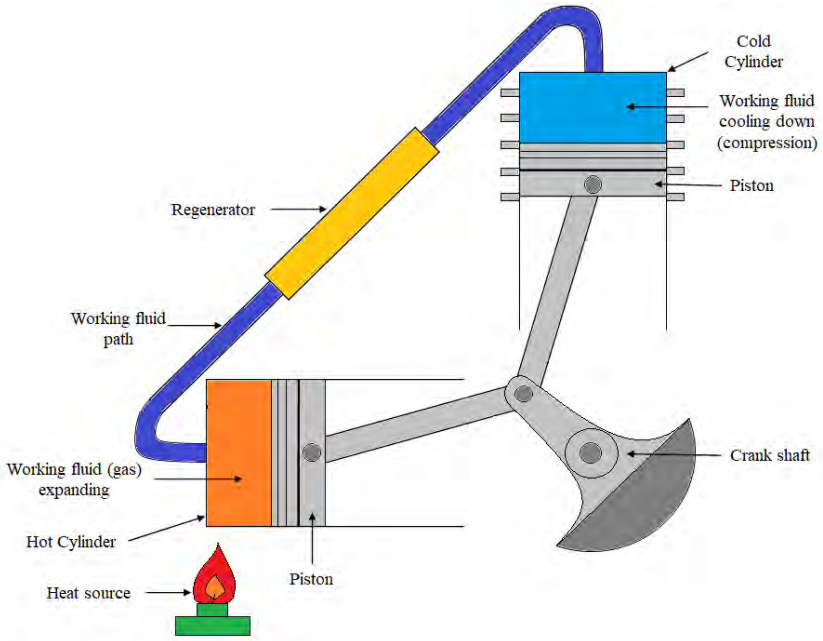

Fig1: The Stirling engine

2.3 Solar Water Heater

The sole purpose of these systems is to generate hot water using solar energy (Ogueke et al., 2009). Solar water heating systems can be broadly classified into active and passive categories. Active solar heating is when the water/heat transfer fluid is pumped from the storage tank through the collectors and back into the tank. Passive systems use natural convection to circulate heated household water/heat transfer fluid. Solar water heaters can be further divided into **direct** and indirect systems. In a direct system, the working fluid passing through the solar panel is the end-use fluid. In contrast, in an indirect system, the working fluid in this system is called a heat transfer fluid and circulates through a solar panel and then goes to the storage tank to exchange heat with the end-use fluid (Ogueke et al. 2009; Bayoumi et al. 2021; Samo et al. 2012).

3. METHODOLOGY

The simulated Stirling engine and solar water heater were based on real-world parts purchased at any hardware and auto-spares retail outlet. The empirical data collected during the experiment were analysed to determine the peak power rating of the engine in watts as well as the backup time in hours. The experiment results were used to design similar-sized solar PV systems with different battery backup systems: deep-cycle gel and lithium iron phosphate. This information was then used to find prices for all the PV equipment and compared to the overall costs associated with the Stirling system.

3.1 Proposed Materials and Parts for the MATLAB Model

To design a large bore engine, the selected pistons belong to Toyota's 2TR-FE engine and have a cross-sectional diameter of 95 mm. The conrods, crank arms and base are modelled out of 25 x 25 mm mild-steel square tubing, owing to the following factors: easily accessible, economical, high tensile strength

and easier to work with than other materials like aluminium. Static balancing will be done on the crankshaft by ensuring that the counterweight equals 100% of the mass of the rotating parts and 50% of the mass of the reciprocating parts. The only drawback of using mild steel is the increased overall weight of the engine and requiring higher starting power input due to increased inertia. Standard-sized bearings, pullies and belts will be used in the drive train. The cylinders are stock machined to accommodate the pistons and have an overall length of 210 mm. The regenerator will accommodate a brass kitchen sponge inside a thermal-resistant container. The solar water heater tank was modelled after a refurbished 210 ℓ steel drum, and the solar collector tubes will be black HPE PVC irrigation pipes with an outer diameter of 50 mm and wall thickness of 2 mm. Each collector tube will be 1.8 m long, and there will be 5 pairs running parallel to and from the water tank. A galvanised IBR sheet will have the dual function of providing structural support while also reflecting solar energy to the collector tubes. All areas that require thermal insulation will be covered by commercially available glass wool of 100 mm thickness.

3.2 Mathematical Model

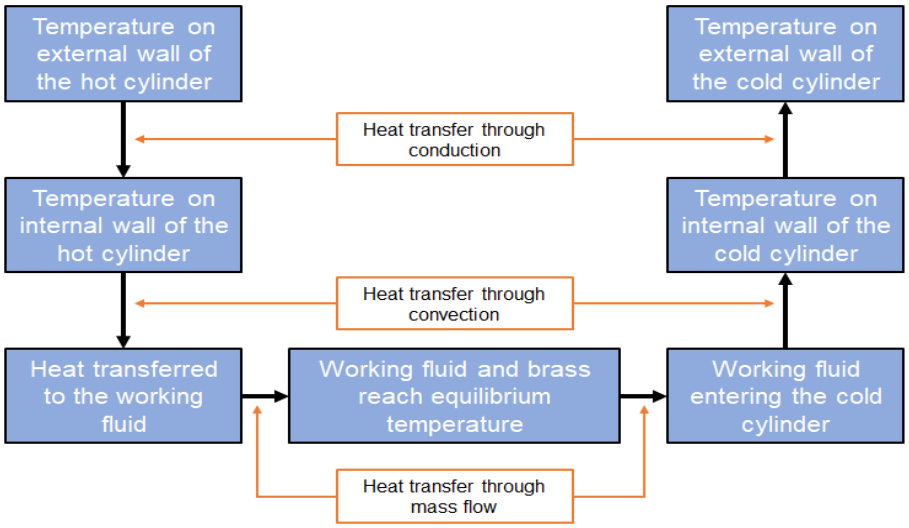

Fig 2: The heat flow model flow chart

The heat flow model is depicted in Fig 2. The Stirling engine was studied by examining the heat transfer mode of each part of the engine. The heat transfer model considers the thermal energy that flows in and out of the engine. The heat flow is transferred to the working fluid via the heat exchangers at the hot and cold sides. The internal heat transfer model is calculated using heat transfer correlations for steady-state internal forced convective flow for the hot and cold cylinders (Araoz et al. 2014). Mass flow equations analyse the regenerator by assuming that the air inside the regenerator and the brass wool is in thermal equilibrium.

Once all the internal temperatures and pressures were calculated, the maximum available output was obtained using the ideal gas equations. The pumping loss was also calculated and subtracted from the maximum available output. The mechanical losses were treated as constant and inferred from online research instead of being calculated.

3.2.1 Heat flow in the hot and cold cylinders

The conduction heat transfer through the wall follows the Fourier law of conduction, while the convection heat transfer rate is consistent with Newton´s cooling Law (Araoz et al. 2014). This can be expressed in terms of the thermal resistance of each mode, i.e., conduction through the wall and

convection through the air surrounding the wall. The total heat energy entering the hot cylinder is expressed as:

$$Q_{hot\_in} = \frac{(T_{hot\_cyl\_outer} - T_{hot\_air\_inner})}{(R_{cond\_hot\_cyl} + R_{conv\_Hot\_cyl})} \quad (1)$$

Where $T_{hot\_cyl\_outer}$ and $T_{hot\_air\_inner}$ represent the outer surface temperature and inner air temperature of the hot cylinder in Kelvin respectively. $R_{cond\_hot\_cyl}$ is the conduction resistance of the cylinder wall while $R_{conv\_Hot\_cyl}$ is the convection resistance of the air inside the cylinder. The conduction and convection resistances of a cylindrically shaped wall are given by:

$$R_{cond} = \frac{\ln\left(r_{inner}/r_{outer}\right)}{K_{mat}.2.\pi.L} \quad (2)$$

$$R_{conv} = \frac{1}{.(r_{in}\ or\ r_{out})} \quad (3)$$

Where K_{mat} is the conductivity of the wall material and h_{liquid} is the convection coefficient of the liquid or gas flowing around the wall surface. The variables r_{inner} and r_{outer} represent the inner and outer diameter of the cylinder wall. Equations (1) to (3) can also be used to solve the heat transfer model of the cold cylinder, as the heat transfer model out of the cold cylinder is exactly the same as the heat transfer model for the heat energy entering the hot cylinder, except that flow direction of flow is heat out instead of heat in.

3.2.2 Heat transfer model of the regenerator

The regenerator material's physical mass and gas need to be established to solve the regenerator's heat transfer model. The brass was weighed on a kitchen scale, while the mass of the gas was calculated using the following equations:

$$P.V = m.R.T \quad (4)$$

Where:
P = Pressure in Pascal
V = Volume in m³
m = Weight in kg
R = Specific gas constant of the working fluid in J/kg.K
T = Temperature of the working fluid in Kelvin

For the mass flow calculations, the gas inside the regenerator is assumed to be in thermal equilibrium with the brass wool. This means that the heat energy "lost" by the working fluid equals the heat energy "gained" by the brass wool.

$$m_{gas}.C_{p_{gas}}.\left(T_{gas} - T_{regen}\right) = -m_{brass}.C_{p_{brass}}.\left(T_{regen} - T_{brass}\right) \quad (5)$$

The variables m, C_p and T represent the mass, specific heat constant and absolute temperature of the materials, respectively. The subscripts represent the two materials in question: the working fluid (gas) and the regenerator material (brass).

Re-arranging equation (5):

$$T_{regen} = \frac{(m_{gas}.C_{p_{gas}}.T_{gas})+(m_{brass}.C_{p_{brass}}.T_{brass})}{(m_{gas}.C_{p_{gas}})+(m_{brass}.C_{p_{brass}})} \quad (6)$$

3.2.3 Pumping loss

Gas flow generates a pressure drop across the regenerator matrix resulting in loss of piston work and decreasing the overall performance (Ishii et al. 2015). To calculate the pressure-drop, the friction coefficient of the regenerator pipe must first be established. This is achieved by calculating the volumetric flow inside the generator:

$$Q_{flow} = \frac{(\pi.D^4.\Delta P)}{(128.\mu.L)} \quad (7)$$

Where:

Q_{flow} = Volumetric flow in m^3/s
D = Diameter of the pipe in meters
ΔP = Differential pressure of the system in Pascal
μ = Dynamic viscosity of the working fluid in Pa.s
L = Length of the pipe in meters

The velocity of the working gas in m/s can be inferred by:

$$V = \frac{Q_{flow}}{\left(\frac{\pi}{4}\right).D^2} \quad (8)$$

From the velocity, the Reynolds number can be obtained:

$$R_e = \frac{\rho.D.V}{\mu} \quad (9)$$

Where ρ is the density of the working fluid in kg/m^3.

For flow in a pipe of diameter D, the flow is turbulent if the Reynolds number is greater than 2300. If the Reynolds number is less than 2300, the flow is laminar, and the friction coefficient is given by:

$$f = \frac{64}{R_e} \quad (10)$$

Using the friction factor obtained in equation (10), the pressure drop across the regenerator will be determined by:

$$J = \frac{f.L.V^2}{2.g.D} \tag{11}$$

Where g represents the gravitational acceleration of earth as 9.81 m/s². As the working fluid flows through the regenerator twice for each cycle, the pumping loss will be:

$$W_{pump\_regen} = 2.J.\Delta V \tag{12}$$

Where ΔV represents the differential volume in m³ through which the working fluid must flow. The pressure drops across the regenerator account for 70% to 90% of the pressure drop through the heat transfer components (Araoz et al. 2014). Thus, the total pumping loss becomes:

$$W_{pump\_total} = \frac{W_{pump\_regen}}{0.7} \tag{13}$$

3.2.4 Crank angle vs piston stroke

Stirling engines are by design valveless, and the hot and cold cylinders are directly connected via the regenerator. This means that calculating the minimum and maximum volumes of the engine is not as simple as deducting the full stroke volume from the compression space volume. To establish minimum and maximum volume, the piston stroke position must be obtained with respect to the crank angle. This can be done by using Pythagorean trigonometry as shown below:

$$x = r.cosA + \sqrt{(L^2 - r^2.sinA^2)} \tag{14}$$

Where x is the piston position with respect to the bottom dead centre and r represent the length of the crank arm. L and A represent the conrod length and the crank angle respectively.

Figure 3 shows the relationship between the hot and cold piston with relation to the crank angle.

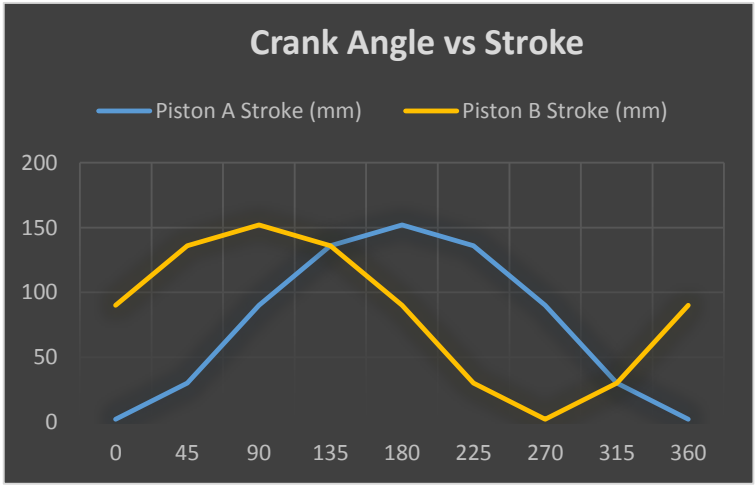

Fig 3: Graph depicting crank angle vs stroke for both pistons

3.2.5 Net-work output of the Stirling engine

To determine the net-work output of the engine, the work done by the hot and cold cylinders must be added together, while the pumping loss and mechanical losses need to be subtracted, as shown in equation (15).

$$W_{out} = P_{hot}.\Delta V + P_{cold}.\Delta V - W_{pump\_total} - W_{mech\_loss} \quad (15)$$

The mechanical efficiency of a four stoke engine is approximately 80% to 90% (Mohammed et al. 2015). Thus, the mechanical loss will be taken as 20% of the break work done by the engine.

3.2.6 Solar collector model

The peak sun hour method was used to estimate the total solar energy entering the collector. The definition of a peak sun hour is the equivalent number of hours per day when solar irradiance averages 1 000 W/m² (Riza & Gilani, 2014). According to the Department of Energy of South Africa, the average peak sun hours in South Africa are between 4.5 to 6.5 hours per day.

Determining the total maximum energy received by the collector:

$$Q_{solar\_in} = 1000.Surface\ area\ of\ the\ collector \quad (16)$$

The heat flow of the solar collector is shown in Figure 2.3, where the green arrows represent conduction heat transfer and the blue arrows show the convection heat transfer for each part of the collector.

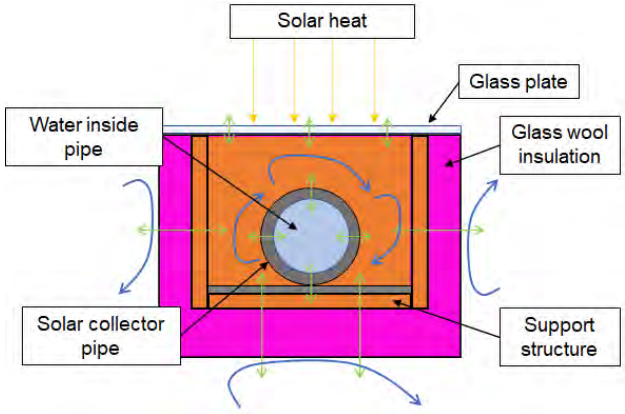

Fig 4: Cross-sectional area for a solar collector with a single pipe

Using figure 4, equation (1) and (16), the heat transfer model will be:

$$Q_{sol\_in} = \frac{(T_{col\_water} - T_{solar\_in})}{(R_{cd\_gl} + R_{cv\_in} + R_{cd\_p} + R_{cv\_p\_in} + R_{cd\_ins} + R_{cv\_ins})} \quad (17)$$

Where:

T_{col_water} = Water temperature inside the collector pipe in Kelvin
T_{solar_in} = Ambient Temperature in Kelvin
R_{cd_gl} = Conductive resistance of the glass cover

R_{cv_in} = Convective resistance of the space around the collector pipes
R_{cd_p} = Conductive resistance of the collector pipe wall
$R_{cv\_p\_in}$ = Convective resistance of the water inside the collector pipe
R_{cd_ins} = Conductive resistance through the insulation wall
R_{cv_ins} = Convective resistance of the air over the insulation wall

Re-arranging equation (17) to solve for the water temperature inside the collector pipe:

$$T_{col\_water} = Q_{sol\_in}.(R_{cd\_gl} + R_{cv\_in} + R_{cd\_p} + R_{cv\_p\_in} + R_{cd\_ins} + R_{cv\_ins}) + T_{solar\_in} \quad (18)$$

3.2.7 Hot water - Stirling heat transfer interaction

To determine the backup hours of the hot water system, the thermal efficiency and the engine's output energy need to be established. Using MATLAB Simulink, the final temperature inside the hot water tank can be established as well as the time the hot water can keep the engine running at night. Equations (19) to (25) were used to establish parameters to be inserted into the Simulink program.

Thermal efficiency of Stirling engine at night:

$$\eta_{Thermal\_night} = \frac{T_{tank} - T_{ambient\_night}}{T_{tank}} \quad (19)$$

Output work of the engine at night:

$$W_{out\_night} = P_{hot\_night}.\Delta V + P_{cold\_night}.\Delta V - W_{pump\_total} - W_{mech\_loss} \quad (20)$$

Input energy needed from the hot water:

$$W_{in\_night} = \frac{W_{out\_night}}{\eta_{Thermal\_night}} \quad (21)$$

Mass of the hot water that needs to be in contact with the heat transfer area:

$$Mass_{water} = \frac{W_{in\_night}}{(Cp_{water} * (T_{tank} - T_{ambient\_night})} \quad (22)$$

Water flow in litres per minute:

$$Flow = Mass_{water}.60 \quad (23)$$

The lowest amount of input energy needed to overcome engine losses:

$$W_{min} = W_{pump\_total} + W_{mech\_loss} \quad (24)$$

Lowest temperature the hot water tank may go and still produce output power:

$$T_{tank\_min} = \frac{(W_{min} - (C_{p_{water}} \times Mass_{water} \times T_{tank}))}{(C_{p_{water}} \times Mass_{water})} \quad (25)$$

3.3 Software Model

This research makes use of MATLAB R2018a a powerful software program to simulate each part and sub-system of the whole machine to calculate its performance. Figure 5 shows the different parts and how they are integrated to form the entire system.

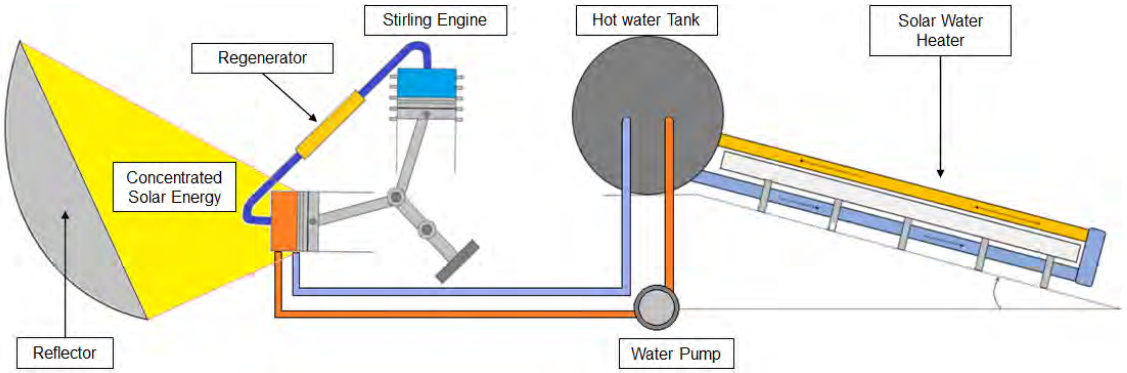

Fig 5: Overall layout of the system

3.3.1 Stirling engine simulation

Figure 6 shows the Simulink model of the Stirling engine. The Simulink model consists of various function blocks and so-called "solid" blocks. Each solid block represents a single component of the Stirling engine, while the function blocks perform specific functions within the program and dictate how these solids interact with one-another. These blocks are connected in specific ways to form a complete three-dimensional object that can be simulated.

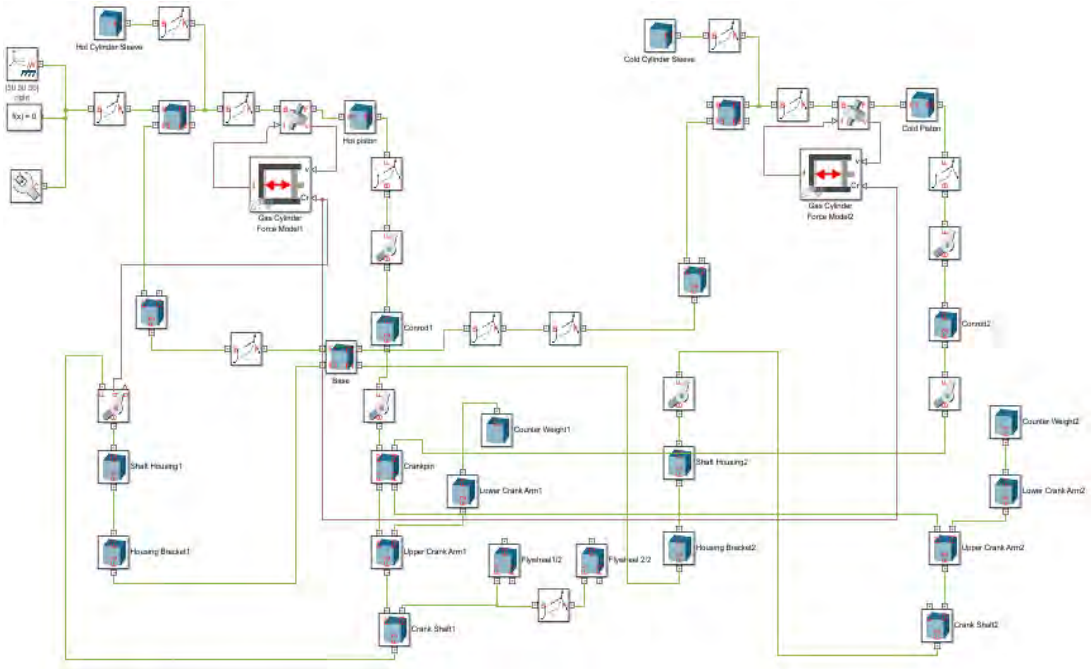

Fig 6: Simulink model of the Stirling engine

The geometry, weight, orientation and connections of each component can be programmed in these solid blocks. Figure 7 is the solid block representing the piston of the hot cylinder in the Stirling engine and is based on the Toyota 2TR-FE piston.

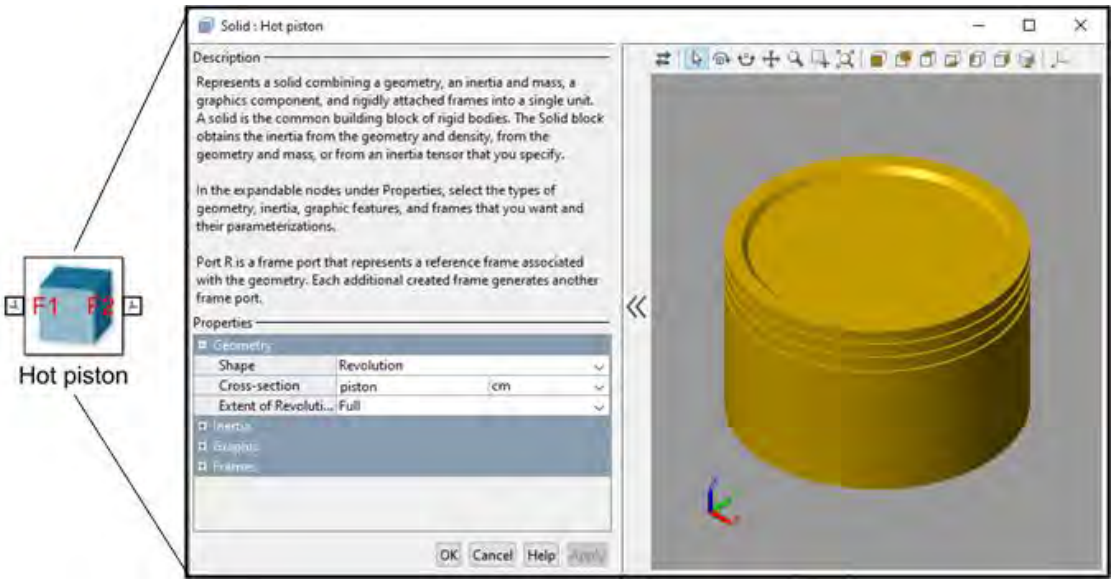

Fig 7: Simulated piston head

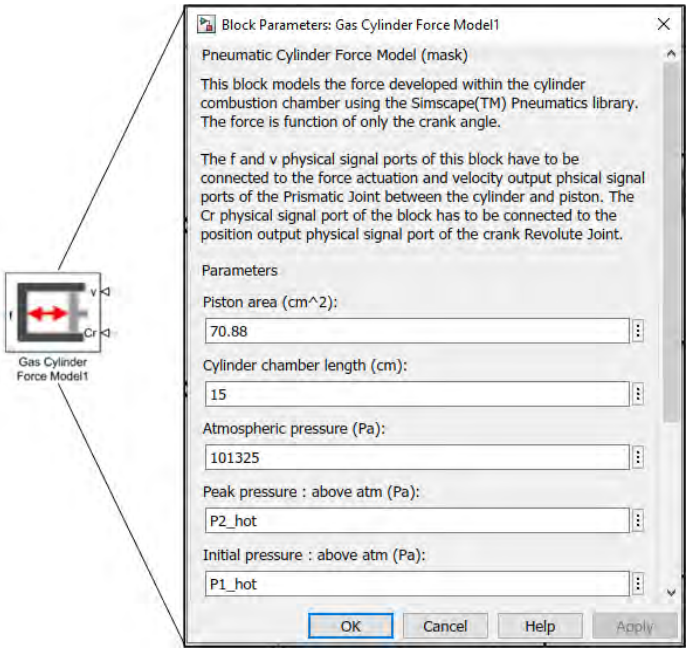

Fig 8: Gas cylinder force model

The gas cylinder force model (see figure 8) is responsible for simulating the force developed within the cylinder combustion chamber using the Simscape Pneumatics library. The force is a function of the crank angle. The “f” and “v” physical signal ports of this block must be connected to the force actuation and velocity output physical signal ports of the prismatic joint between the cylinder and piston. The “Cr” physical signal port of the block must be connected to the position output physical signal port of the crank revolute joint. The physical dimensions of the bore and stroke of the piston are plugged into the parameters, while the initial and maximum pressures are derived from the mathematical model. Figure

9 shows the assembled Stirling engine based on the Simulink model, complete with crankshaft, flywheel, pistons, conrods and cylinders. The regenerator is not included in the Simulink model as it forms part of the mathematical model.

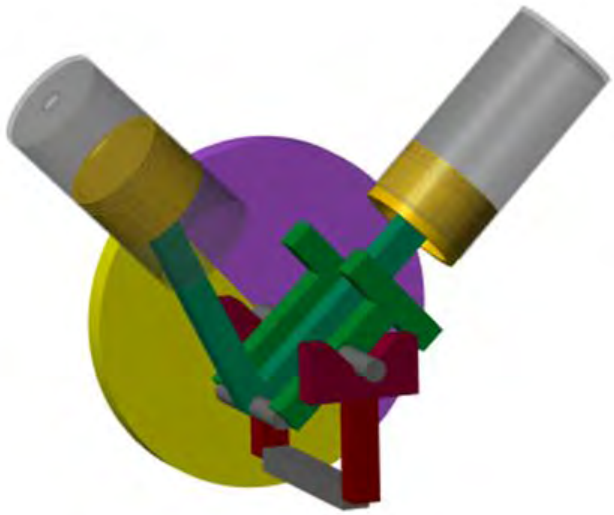

Fig 9: Simulated Stirling engine

3.3.2 Solar hot water system simulation

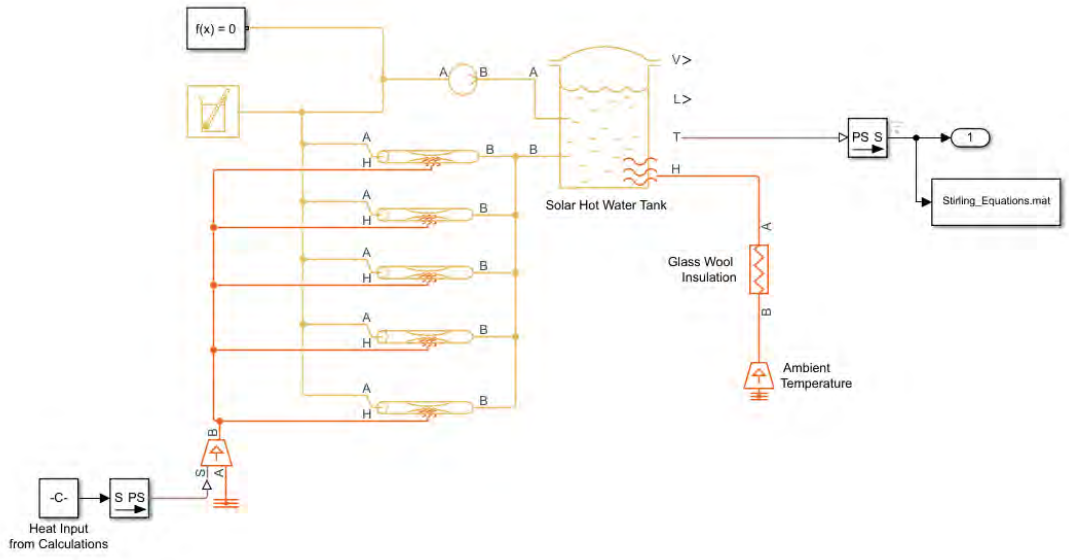

Fig 10: Simulink model of solar hot water system

The solar hot water system was created using MATLAB Simulink, shown in Figure 10. This model is designed to emulate a physical solar water heater in the sense that heat energy is transferred to the water through the walls of several pipes called collectors. Like the Stirling model, each block represents either; a physical component or a specific function and can be programmed as depicted in Fig 11 and Fig 12.

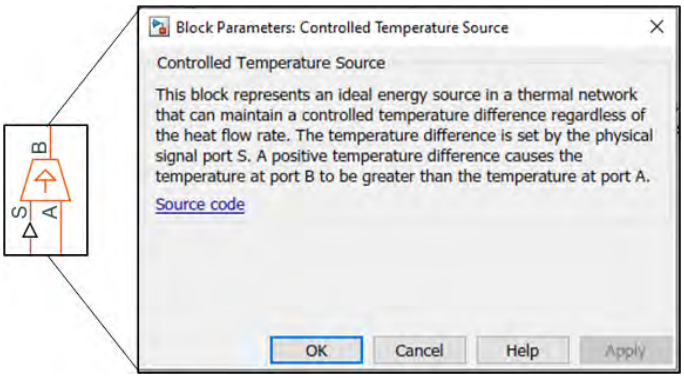

Fig 11: Example of a typical function block

This heated water is then stored inside an insulated water tank for later use. The input block labelled "C" in Figure 10 derives its value from the mathematical model of the solar hot water equations, while the system output is connected to the Stirling equations represented by the function block labelled "Stirling_Equations.mat". The simulation of the hot water tank is shown in figure 11 and displays all the parameters which can be programmed to simulate the temperature inside accurately.

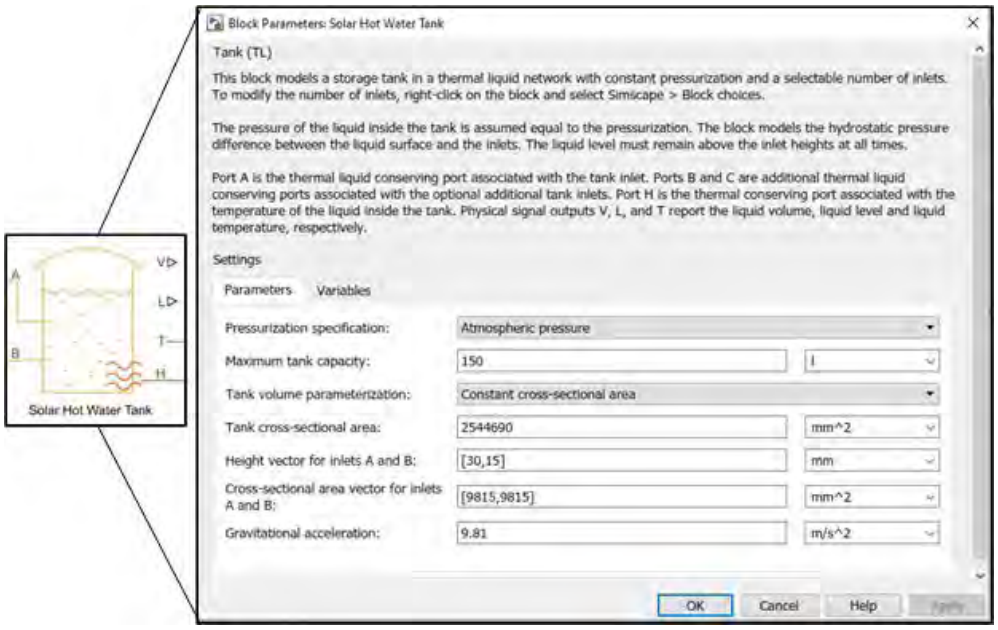

Fig 12: Simulation of the hot water tank

3.3.3 Hot water - Stirling interface simulation

This system was also created using MATLAB Simulink and simulates the interaction between the hot water tank and the Stirling engine at night. This simulation takes the hot water inside the tank and circulates it through the contact area between the hot piston and the hot water. The heat is then transferred to the air inside the Stirling engine through conduction and convection, as shown in Figure 13. This process continues until the temperature inside the water tank reaches the low-temperature limit derived from equation 25.

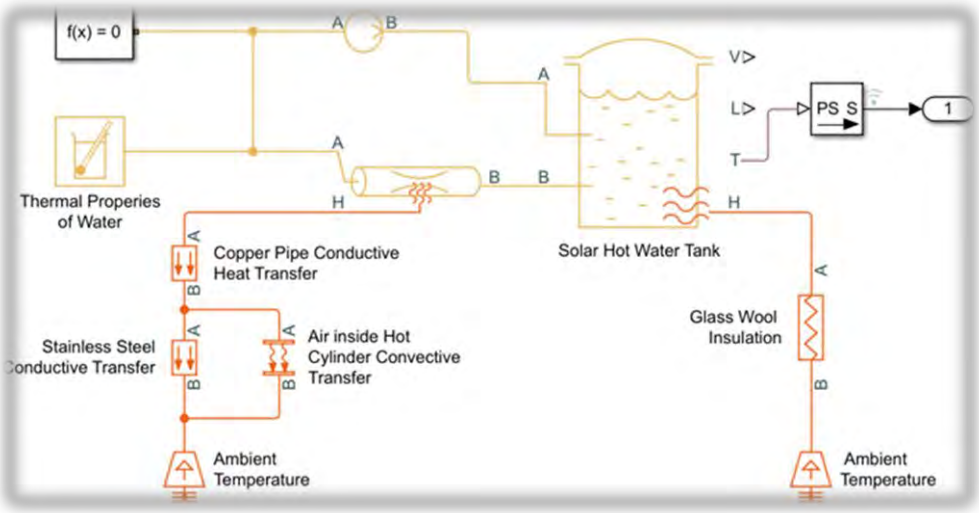

Fig 13: Simulink model of the interface between the Stirling engine and hot water

4. RESULTS

Certain conditions need to be implied before any equations or simulations can be done. These conditions are described in Table 1 and includes the focussed solar temperature on the Stirling receiver, the temperature in the shade (in the case of the cold cylinder) and the ambient temperature at night.

Table 1: Input temperatures

Concentrated Solar in	100°C
Ambient (shade)	25°C
Ambient (night)	17°C

Air will be chosen as the working fluid inside the Stirling engine and the internal system pressure is raised to 200 kPa; thus, the thermal properties of air will be used. Table 2 depicts the list of thermal properties of air – each with its corresponding value to be used in the mathematical model.

Table 2: Thermal properties of air

Properties of air	Value	Unit
Density	1.225	kg/m³
Dynamic Viscosity	0.0018	Pa.s
Convection (free air)	50	W/m².K
Convection (forced air)	100	W/m².K
Specific gas constant	287	J/kg K
Specific heat capacity	1 000	J/kg.K

Table 3 contains a list of materials used in the simulation and depicts the conductivity constants for each of them. Materials like stainless steel and copper are used to transfer heat more effectively as they have high conductivities, while glass wool was used to insulate certain parts due to its low conductivity.

Specific heat capacity of thermal storage material (water) and regenerator material:

C_{p_water} = 4200 J/kg.K

C_{p_brass} = 920 J/kg.K

The engine stroke is taken as 150 mm and the bore is 95 mm, the generator is accepted to have an overall efficiency of 80% and the volume of water inside the tank is taken as 100 litres.

Table 3: Thermal conductivity of selected materials (W/m.°K)

Stainless steel	16.2
Copper	399
Glass wool	0.03
Glass	0.02
PVC	0.16

4.1 Stirling Engine Output Result

Figure 14 shows the result obtained from the MATLAB editor for both the mechanical and electrical power generated by the Stirling engine. Line 162 is the MATLAB editor's equivalent for equation 15.

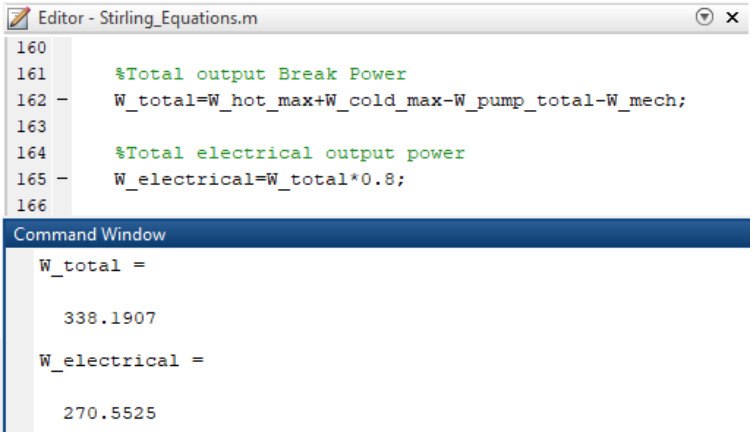

Fig 14: Simulated power output of the Stirling engine

4.2 Simulated Maximum Water Temperature

The simulated maximum water temperature inside the water tank is depicted in Figure 15. The final temperature inside the water tank will be 333 degrees Kelvin or 60 degrees Celsius. The simulation was run for 5 hours, as the literature review suggests South Africa receives around 5 hours of peak sunlight hours per day.

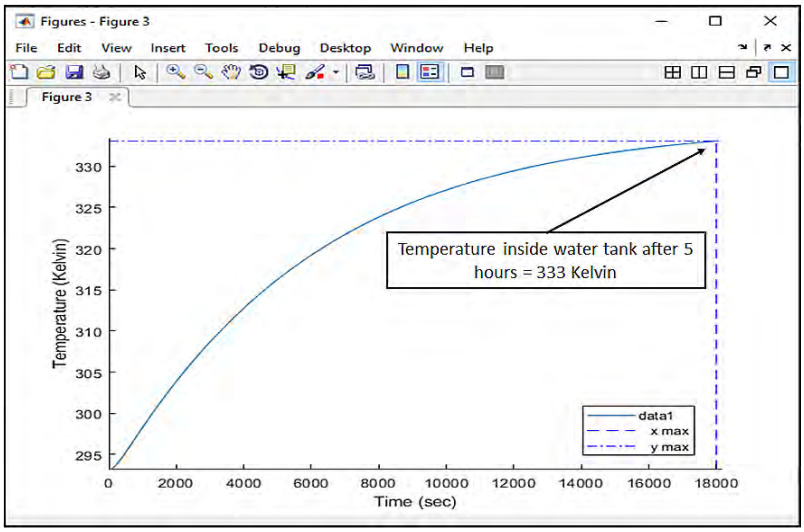

Fig 15: Simulated maximum water temperature inside the tank after 5 hours of peak sunlight

4.3 Simulated Total Backup Time

The simulated total backup time that the Stirling engine can run at night is shown in Figure 16 and is equal to 3.278 hours. The minimum temperature for the water is calculated to be 311.6 Kelvin (38.6 °C) based on equation 25 and is the least amount of heat energy needed to overcome the engine losses as calculated by equation 24.

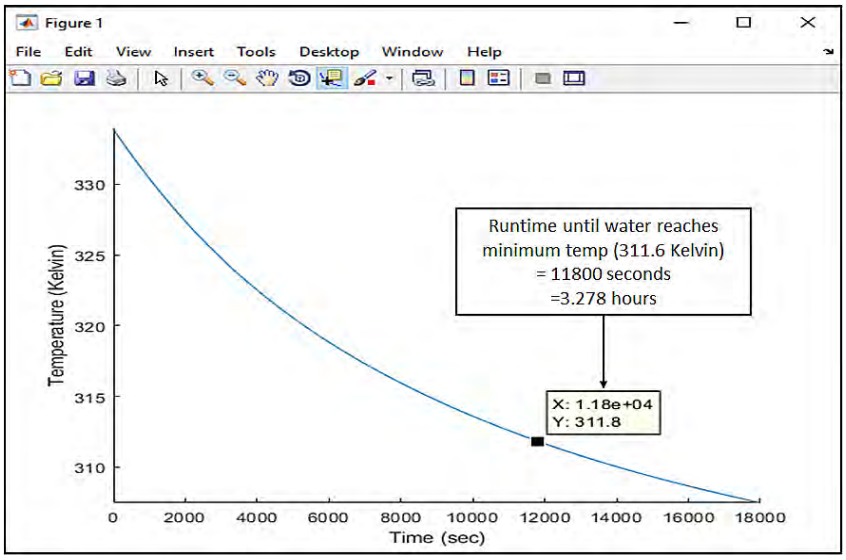

Fig 16: Simulated total backup time for the Stirling engine running at night

4.4 Findings

The solar PV systems need to be able to deliver 270 Watts of electricity during the day, while the battery backup system needs to supply the load for at least 3 hours and 16 minutes.

Table 4: Tabulated results from simulations

Maximum electrical output (Watts)	270.55
Maximum water temperature (Kelvin)	333
Backup time (Hours)	3.28

Based on the results shown in Table 4, the equivalent solar PV system would need: one 365-Watt PV panel, one 400-Watt pure sine wave inverter, one 12 Volt, 40 Amp-hour deep-cycle gel battery, or one 12 Volt, 22 Amp-hour lithium iron phosphate battery. This information was used to develop comprehensive bills of material for the 2 proposed PV systems. From the bill of material, the overall cost of assembling such a system was inferred.

5. INTERPRETATION OF RESULTS

Based on the results gathered, comprehensive bills of material (BOM) for the two systems could be generated. Table 5 depicts the BOMs for PV solar with deep-cycle gel battery and for PV solar with lithium iron phosphate battery backup respectively. The parts are listed on the left-side column, the quantity of each corresponding part in the middle column and the price for each corresponding item in the right-side column. The grand total is displayed at the bottom and is the sum of all the prices listed in the right-side column.

Table 5: Bill of material for PV solar with deep-cycle gel battery and lithium iron phosphate battery

Description	Quantity	Price with deep-cycle gel battery	Price with lithium iron phosphate battery
JA Solar 365-Watt mono solar panel	1	R3 330.00	R3 330.00
400-Watt Victron inverter	1	R2 220.00	R2 220.00
Victron smart solar MPPT 75/15	1	R2 510.00	R2 510.00
12 Volt, 40 Ah, gel battery	1	R1 850.00	R2 460.00
6mm² red solar cable (per meter)	10	R180.40	R180.40
6mm² black solar cable (per meter)	10	R180.40	R180.40
MC 4 connector (per pair)	2	R110.00	R110.00
Solar panel roof bracket	1	R120.00	R120.00
TOTAL		R10 500.80	R11 110.80

As mentioned, the simulated Stirling engine and solar water heater was based on real-world parts. The parts and their prices are listed in Table 6 and shows that the Stirling engine would cost R9 875.86 to build.

Table 6: Bill of material for solar powered Stirling engine with thermal stored energy

Part Description	Qty	Supplier	Price Each	Line Total
2TR-FE Toyota Engine Piston (incl. rings and pins)	2	Midas	R552.00	R1 104.00
Steel Sleeves, ID:95mm, OD:99mm, L:212mm	2	Ferro-Tech	R736.00	R1 472.00
Ball Bearing, ID:8mm, OD:22mm, W:7mm	4	BMG	R22.50	R90.00
Ball Bearing, ID:20mm, OD:42mm, W:12mm	4	BMG	R64.60	R258.40
25mm Mild Steel Square Tubing per length (6 meters)	1	Stewards & Lloyds	R203.55	R203.55
Refurbished 210l Steel Drum with lid	1	Amtec	R159.85	R159.85
100kPA Pressure Safety Relief Valve	1	Buco	R509.00	R509.00
Glass Wool (Aero-Lite) 135mm x 1.2M x 5M	1	Leroy-Merlin	R598.00	R598.00
22mm Rubber Hose per meter	1	HoseWorld	R80.50	R80.50
22mm Copper Pipe per length (4 meters)	1	Leroy-Merlin	R429.00	R429.00
50mm HDPE Black Irrigation Pipe per meter	40	Builders Warehouse	R42.00	R1 680.00
PVC Bend, 50mm, 90 Degrees	20	Leroy-Merlin	R19.90	R398.00
IBR galvanised Roof sheet (0.4 x 686 x 3200mm)	1	Stewards & Lloyds	R373.45	R373.45
12V DC Water Pump (20-30Watt)	1	Takealot	R649.00	R649.00
Angle Grinder, 230V, 850W	1	Adendorff	R595.00	R595.00
600V, 25Amp Bridge Rectifier	1	RS Components	R45.00	R45.00
Day/Night Switch, 6A	1	Builders Warehouse	98.00	98.00
U-Bolt, 50mm x 8mm	2	Builders Warehouse	R35.00	R70.00
M20 Stud Bolt, 195mm, Partially Threaded	1	Benoni Bolt	R86.30	R86.30
M20 Bolt, 110mm, Threaded (25mm)	1	Benoni Bolt	R35.22	R35.22
M20 Bolt, 85mm, Threaded (25mm)	1	Benoni Bolt	R30.05	R30.05

M20 Nut	6	Benoni Bolt	R5.75	R34.50
M20 Flat Washer	10	Benoni Bolt	R0.87	R8.70
M20 Spring Washer	6	Benoni Bolt	R2.22	R13.32
Fenner Friction Belt, V-Wedge, 13 x 8 x 1610mm	1	BMG	R44.62	R44.62
SPA Fenner Pulley 80mm	1	BMG	R77.60	R77.60
SPA Fenner Pulley 315mm	1	BMG	R572.00	R572.00
Fenner Taper Lock Bush 1210x20	1	BMG	R61.00	R61.00
Fenner Taper Lock Bush 2012x20	1	BMG	R99.80	R99.80
TOTAL				R9 875.86

6. CONCLUSION

From the results, it is plausible that a solar-powered Stirling engine with sensible heat energy backup can be designed and built as an alternative to solar PV systems for the generation of power at a lower capital cost. It is clear from Table 7 that the Stirling engine is cheaper than both types of solar PV systems.

Table 7: Price comparison between the 3 proposed systems - listed from low to high

System Type	Capital Cost (Rand)	Percentage Difference (%)
Solar Stirling engine with stored thermal energy backup	R9 875.86	-
Solar PV with deep-cycle gel backup	R10 500.80	6
Solar PV with lithium iron phosphate backup	R11 110.80	11

ACKNOWLEDGEMENTS

Name Affiliation
Dr G. Sutherland Vaal University of Technology
Dr A. Joubert Vaal University of Technology
Prof. J. Bekker Vaal University of Technology
Assoc. Prof. W. le Roux University of Pretoria
Pr. H. Fourie ArcelorMittal South Africa

REFERENCES

Alalewi, A. Concentrated Solar Power (CSP), https://www.researchgate.net/publication/262178578_Concentrated_Solar_Power_CSP; 2014 [accessed: 28 July 2022].

Araoz, J. Salomon, M. Alejo, L. and Fransson, T. Non-Ideal Stirling Engine Thermodynamic Model Suitable for the Integration into Overall Energy Systems. Applied Thermal Engineering, 2014; 73(1): 203-219. DOI: 10.1016/j.applthermaleng.2014.07.050.

Bayoumi, S. and Moharram, N. Concentrated Solar Power Part 1: Introduction, https://www.researchgate.net/publication/350076164_Concentrated_Solar_Power_Part_1_Introduction; 2021 [accessed: 03 August 2022].

Chivandire, K. 2020. Is solar power the answer to Southern Africa's energy crisis, https://mg.co.za/business/2020-10-14-is-solar-power-the-answer-to-southern-africas-energy-crisis/; 2020 [accessed: 10 June 2022].

Department of Energy – South Africa, How Does Solar Work? https://www.energy.gov/eere/solar/how-does-solar-work; n.d. [accessed: 26 May 2022].

Hagumimana, N. Zheng, J. Asemota, G. N. O. Niyonteze, J. D. D. Nsengiyumva, W. Nduwamungu, A. and Bimenyimana, S. Concentrated Solar Power and Photovoltaic Systems: A New Approach to Boost Sustainable Energy for All (Se4all) in Rwanda. International Journal of Photoenergy, 2021; 1-32. DOI: 10.1155/3837.

Hughes, M. Why access to energy should be a basic human right. Forbes, https://www.forbes.com/sites/mikehughes1/2018/12/10/why-access-to-energy-should-be-a-basic-human-right/?sh=e3208d45f2ee; 2018 [accessed: 20 June 2022].

Ishii, H. Bouzawa, D. and Hamaguchi, K. Heat transfer characteristics and pressure drop of high-porosity regenerator matrix using sintered metal fibre. The Proceedings of the Symposium on Stirling Cycle, Japan, 2015; DOI:10.1299/jsmessc.2015.18.37.

Mannak, M. The Economic Impact of South Africa's Energy Crisis, https://www.africanexponent.com/post/the-economic-impact-of-south-africas-energy-crisis-121; 2015 [accessed: 8 June 2022].

Martini, W. R. Stirling engine design manual. Cleveland: NASA; 1983.

Mileham, K. J. South Africans should not pay for electricity that they do not have, https://www.newsi.co.za/news/south-africans-should-not-pay-for-electricity-that-they-do-not-have; 2022 [accessed: 8 June 2022].

Mohammed, F. Abdallah, M and Taha, M. Measurement of Heat and Mechanical Losses in Internal Combustion Engines. B.Sc. Sudan University of science and technology. http://repository.sustech.edu/bitstream/handle/123456789/12891/Measurement%20of%20Heat%20and%20Mechanical%20Losses%20in%20Internal....pdf?sequence=1; 2015 [accessed: 01 October 2022].

Moolman, S. 2021 update: Eskom tariff increases vs inflation since 1988 (with projections to 2023), https://poweroptimal.com/2021-update-eskom-tariff-increases-vs-inflation-since-1988/; 2021 [accessed: 8 June 2022].

Ogueke, N. V. Anyanwu, E. E. and Ekechukwu, O. V. A review of solar water heating systems. Journal of Renewable and Sustainable Energy, 2009; 1(4): 043106. DOI:10.1063/1.3167285.

Pandarum, A. Lekoloane, G. and Milazi, D. Trends and statistics of Solar PV Distributed Generation in South Africa, https://researchspace.csir.co.za/dspace/bitstream/handle/10204/11033/Trends%20and%20statistics%20of%20Solar%20PV%20Distributed%20Generation%20in%20South%20AfricaTrends%20and%20statistics%20of%20Solar%20PV%20Distributed%20Generation%20in%20South%20Africa%2015082018%20%28clean%29.pdf?sequence=1&isAllowed=y; 2019 [accessed: 8 June 2022].

Pendrid, L. L. ed. The Centenary of the heat regenerator and the Stirling air engine. The Engineer. 124(1): 516. http://hotairengines.org/patents/stirling-patents/THE%20ENGINEER_Stirling's%201816%20patent.pdf; 1917 [accessed: 17 May 2022].

Răboacă, M. S. Badea, G. Enache, A. Filote, C. Răsoi, G. Rata, M. Lavric, A. and Felseghi, R. Concentrating Solar Power Technologies. Energies, 2019; 12(6): 1048-6. DOI:10.3390/en12061048.

Rinker, G. T. Design and Optimization of a 1 kW Stirling Engine. PhD. West Virginia University, https://researchrepository.wvu.edu/cgi/viewcontent.cgi?article=4689&context=etd; 2018 [accessed: 3 February 2022].

Riza, D. F. A. Gilani S. I. H. Standalone photovoltaic system sizing using peak sun hour method and evaluation by TRNSYS simulation. International Journal of Renewable Energy Research. 2014; 4(1):109-114. DOI: 10.1155/ijer.

Samo, S. R. Siyal, A. A. Siyal, Z.A. and Jatoi, A. R. Analysis of an Active and Passive Solar Water Heating System. IWTC 16 2012: Sixteenth International Water Technology Conference, Istanbul, Turkey, 7-10 May 2011, https://www.researchgate.net/publication/316854104_ANALYSIS_OF_AN_ACTIVE_AND_PASSIVE_SOLAR_WATER_HEATING_SYSTEM; 2011 [accessed: 29 June 2022].

Toussaint, K. The price of solar electricity has dropped 89% in 10 years, https://www.fastcompany.com/90583426/the-price-of-solar-electricity-has-dropped-89-in-10-years; 2020 [accessed: 10 June 2022].

Walker, G. Stirling Engines. Oxford: Clarendon Press, Oxford University Press; 1980.